SUPPPLEMENTARY MATERIALS

Materials and Methods

Figs. S1 to S6

Materials and Methods

Molecular techniques

Plasmid constructions, protein analysis by SDS-PAGE and immunoblotting, siRNA-mediated protein depletion, and cell proliferation analysis used standard methods.

Recombinant GST-Elk-1 TAD.

Wild-type or mutant mouse Elk-1 sequences encoding residues 309-429 were expressed as GST-$(His)_6$ fusion proteins, inserted between BamHI and NotI sites of modified pET-41a (*30*). Protein expression was induced in *E. coli* BL21(DE3) (Novagen) with 0.5 mM IPTG at 37° C. Cells were lysed in 50 mM Tris pH 8.0, 300 mM NaCl, 5 mM DTT, with Complete protease inhibitor cocktail (Roche Diagnostics). Cleared lysates were applied to glutathione Sepharose resin (GE Healthcare Life Sciences) and washed extensively with lysis buffer. Proteins were eluted with 20mM reduced glutathione in 50 mM Tris pH 8.0, 150 mM NaCl, 5mM DTT, and further purified on a Superdex 200 HR10/30 size exclusion column (GE Healthcare Life Sciences) in 20 mM K_2HPO_4 pH 6.8, 150 mM NaCl, 5 mM DTT. For ^{15}N- and ^{15}N-/^{13}C-labeling, growing cells were transferred to minimal medium containing $^{15}NH_4Cl$ and/or ^{13}C-glucose as appropriate and grown at 30 °C. After adsorption to glutathione sepharose the Elk-1 moiety was released by incubation with 1:50 (w/w) GST-3C protease on the resin, and purified by Superdex 75 HR10/30 size exclusion chromatography as above. For phosphorylation, GST-Elk-1 TAD proteins (50μM) were incubated with 400 U ERK2 (NEB) in 100μl 10 mM K_2HPO_4 pH 6.9, 50 mM NaCl, 1 mM ATP, 2mM DTT, 5 mM $MgCl_2$ at 25 °C.

NMR spectroscopy

All NMR experiments were performed on a 750 MHz Bruker NMR spectrometer equipped with cryogenically cooled triple resonance probe (TCI). Resonance assignments for WT and mutant Elk-1 TAD were obtained by 2D ^1H-^{15}N HSQC and 3D HNCACB, HN(CA)CO, CA(CO)NNH, HNCO, (H)N(CA)NH NMR experiments with uniformly ^{15}N- and ^{13}C-labeled samples in 10 mM Na_3PO_4, 50 mM NaCl, pH 6.4, 10% D_2O, at 25 °C. 3D HNCACB experiments were recorded with 512 (t_3) × 64 (t_2) × 42 (t_1) complex data points for ^1H, ^{13}C and ^{15}N dimensions, respectively, HN(CA)CO experiments with 512 (t_3) × 32 (t_2) × 40 (t_1) complex points, CA(CO)NNH experiments with 512 (t_3) × 44 (t_2) × 36 (t_1) complex points, HNCO experiments with 512 (t_3) × 48 (t_2) × 64 (t_1) complex points, (H)N(CA)NH experiments with 512 (t_3) × 44 (t_2) × 44 (t_1) complex points. 2D HSQC experiments were recorded with 512 (t_2) × 128 (t_1) complex points. All 3D NMR spectra were processed with Topspin 3.1 and analyzed in CcpNMR. Final ^1H and ^{15}N amide assignments at pH 6.8 and 298 K were obtained by following progressive cross-peak displacements from pH 6.4 and 277 K to pH 6.4 and 298 K (5 steps: 277 K, 283 K, 288 K, 293 K, 298 K), and from pH 6.4 and 298 K to pH 6.8 and 298 K. Assignments of unmodified and phosphorylated wild-type Elk-1 TAD, as well as details of NMR experiments used to derive them have been deposited in the Biological Magnetic Resonance Data Bank (BMRB, accession numbers 26762 and 26786, respectively).

For time-resolved NMR monitoring of Elk-1 phosphorylation reactions, samples were reconstituted with ^{15}N isotope-labeled Elk-1 TAD (50 μM in 100 μl sample volume 10 mM Na_3PO_4, 50 mM NaCl, 1 mM ATP, 2 mM DTT, 5 mM $MgCl_2$, 10% D_2O, pH 6.9)

and 400 U ERK2 (NEB), or 200 U p38α (Signal Chem), 375 U JNK1, or 375 U JNK2 (both Proqinase) at 25 °C. Progressive phosphorylation was analyzed and quantified as described previously (*20*). Error bars represent the precision with which individual phosphorylation levels were determined for each time point. They reflect the number of uniquely resolved chemical shifts whose peak intensities reported on the modification states of respective ERK2 sites (i.e. phosphorylated serines and threonines, and flanking residues). Intensities of at least two independent NMR signals reporting on the same phosphorylation event were combined for each time point (determined relative to normalized intensities of fully modified sites). Larger error bars represent sites for which fewer signals were combined (= 2), smaller error bars correspond to sites for which greater numbers of peak intensities were integrated (> 2). For measurement points without error bars, the determined experimental precision is smaller than the chosen point size. All time-resolved NMR measurements of individual phosphorylation reactions were repeated on at least two independent replicate samples (n=2) under identical experimental conditions and with the same kinase batch. Error bars reflecting the reproducibility of such measurements are smaller than the chosen point size (ie the circles in the figures; not shown).

Consecutive 2D ^{1}H-^{15}N SOFAST-HQMC experiments were recorded with 64 scans, 40 ms interscan delays, and 512 (t_2) × 64 (t_1) complex points. Individual acquisition times were 15 min and 30 s. All NMR spectra were processed by linear prediction in the ^{15}N dimension (64 complex points), cosine-bell apodization and zero filling to 4,096 (t_2) and 2,048 (t_1) data points, processed with Topspin 3.1 and analyzed in Sparky. Assignment of NMR signals of phosphorylated WT and mutant Elk-1 TAD was based on additional sets of 3D HNCACB experiments and de-novo backbone assignment procedures. Combined ^{1}H and ^{15}N, ^{13}CO chemical shift differences (Δδ) between unmodified and phosphorylated Elk-1 TAD were calculated as $\Delta\delta = [(\Delta\delta_{HN}^2 + (\Delta\delta_{N}*0.154)^2 + (\Delta\delta_{CO}*0.351)^2)^{1/2}]/3$ and plotted for each residue, except prolines (*31*). Secondary structure propensities of unmodified and phosphorylated Elk-1 TAD were obtained with the neighbor-corrected structural propensity calculator (*32, 33*) (http://nmr.chem.rug.nl/cgi-bin/selection_screen_ncSPC.py) using experimentally determined Cα and Cβ chemical shifts as input. Random coil chemical shift values of glycines preceding prolines were corrected to –0.77 p.p.m. according to (*34*). Similarly, random coil chemical shift values of phosphorylated serines and threonines were corrected as outlined in (*35*), also by taking pH-dependent chemical shift changes into account (*36*). Hence, the following correction values were used for chemical shift measurements at pH 6.9: For pSer, $\delta(C\alpha)_{corr} = \delta(C\alpha)+0.012$ and $\delta(C\beta)_{corr} = \delta(C\beta)-1.865$, for pThr, $\delta(C\alpha)_{corr} = \delta(C\alpha)-1.16$ and $\delta(C\beta)_{corr} = \delta(C\beta)-2.33$ (in p.p.m.).

Multisite phosphorylation model

The rate of Elk-1 phosphorylation *in vitro* is dependent on the concentration of ERK2 (fig. S3A), suggesting an apparently distributive phosphorylation mechanism where ERK2 modifies one phosphorylation site per docking encounter with Elk-1 (*37*). Since Elk-1 is released from ERK2 after each phosphorylation step, at each substrate encounter the different phosphorylation sites will effectively compete for ERK2. To simplify the mathematical treatment, we arbitrarily grouped the slower phosphorylation sites according to their distance from the midpoint between the two fastest sites (Fast,

T369 and S384; Intermediate: T354, T364, S389; Slow, T337, T418, S423), with decreasing relative affinities for ERK2 (ie $K_M^{Fast} < K_M^{Int} < K_M^{Slow}$). The phosphorylation kinetics for wild-type Elk-1, with the Fast, Intermediate, and Slow sites were fitted according to equations 1 and 2 (*20, 38*). These equations describe the kinetics for a pair of sites competing for ERK2. As illustrated, equations (1) and (2) represent the relation between the Fast and Slow sites; similar equations can be applied to describe the other pairwise relationships between the different site classes. The δ value, defined in equation 2, indicates the degree of competition between the sites (δ=1 denotes equal competition between sites, while 0<δ<<1 denotes weak competition).

$$\frac{[pS_{fast}](t)}{[S]_{(t=0)}} = 1 - \left(\frac{1 + \frac{[S]_{(t=0)}}{K_M^{slow}}}{\frac{[S]_{(t=0)}}{K_M^{fast}}} * \ln\left(1 + \left[\exp\left(\frac{\frac{[S]_{(t=0)}}{K_M^{fast}}}{1 + \frac{[S]_{(t=0)}}{K_M^{slow}}} \right) - 1 \right] * \exp\left(- \frac{\frac{V_{max}^{fast}}{K_M^{fast}} * t}{1 + \frac{[S]_{(t=0)}}{K_M^{slow}}} \right) \right) \right) \qquad (1)$$

$$\frac{[pS_{slow}](t)}{[S]_{(t=0)}} = 1 - \left(1 - \frac{[pS_{fast}](t)}{[S]_{(t=0)}} \right)^{\delta} \qquad (2)$$

$$\delta = \frac{V_{max}^{slow} \times K_M^{fast}}{K_M^{slow} \times V_{max}^{fast}}$$

Where:
[S] is concentration of the phosphorylation sites; K_M^{Fast}, K_M^{Int} and K_M^{Slow} are the apparent Michaelis-Menten constants for the Fast, Intermediate and Slow groups of sites respectively; V_{max}^{Fast}, V_{max}^{Int} and V_{max}^{Slow} are maximum rates of phosphorylation for the Fast, Intermediate and Slow groups of sites respectively (proportional to the modification turnover rates); δ is the competitive index. Note that Equation 2 is a corrected form (*20, 39*). Complete derivation of these kinetic formulas is published elsewhere (*20, 38*).

The observed data for the wild-type protein were fitted to the competition model in Fig. 2B, left panel, which defined the parameters that determine the δ values as: $\frac{[S]_{(t=0)}}{K_M^{fast}}$ = 12.7, $\frac{[S]_{(t=0)}}{K_M^{int}}$ = 3.34, $\frac{[S]_{(t=0)}}{K_M^{slow}}$ = 2.65, $\frac{V_{max}^{fast}}{K_M^{fast}}$=0.14 min^{-1}, $\frac{V_{max}^{int}}{K_M^{int}}$ = 0.029 min^{-1}, and δ values as: Fast vs Slow, δ = 0.10; Fast vs Int, δ = 0.26; Int vs Slow, δ = 0.43.

The data for the different Elk-1 mutants were then modeled assuming that the competitive relationships between the different types of sites are maintained in the mutants, and that mutated sites have negligible affinity for the kinase. The Elk-1F mutant data fit the model well, with the kinetics of intermediate and slow site phosphorylation in the mutant approaching those of the wild-type fast and intermediate sites respectively (Fig. 2B, center). The Elk-1I mutant data also fitted the model well, with the kinetics of

the fast sites increasing relative to wild-type, and the rate of slow site phosphorylation approaching that of the intermediate sites in wild-type Elk-1 (Fig. 2B, right).

Expression and analysis of wild-type and mutant mouse Elk-1 in triply TCF-deficient MEFs

Triply TCF-deficient (TKO) MEFs, lacking Elk-1, Net, and SAP-1, were prepared from $Elk1^{-/-}$;$Elk3^{\delta/\delta}$;$Elk4^{-/-}$ embryos (*40*) and immortalized using SV40 T antigen (gift from Victoria Lawson). DNA encoding N-terminally flag-tagged full-length wild-type and mutant mouse Elk-1 were synthesized (GeneArt-Life technologies) and expressed using pMIG/MSCV-IRES-GFP (*41*). Cell sorting by GFP was used to isolate populations with similar levels of Elk-1 expression and confirmed by immunoblotting. Elk-1 mutants were: Elk-1F, T369A, S384A; Elk-1I, T354A, T364A, S390A; Elk-1S, T337A, T418A, S423A; Elk-1FI, T354A, T364A, T369A, S384A, S390A; Elk-1FW, F379A, W380A, Elk-1 T418A; Elk-1 S423A; Elk-1 T337A.

For functional analysis, TKO cells expressing wild-type and mutant Elk-1 were grown in triplicate cultures in 6-well plates, serum-starved for 48 h, then stimulated with TPA. For gene expression analysis, RNA was prepared at the time of peak mRNA accumulation (*Egr1*, 45'; *Egr2*, 90'; *Egr3*, 120'; *Fos*, 45'; *Nr4a1*, 60'; *Ier2*, 45'), or over a time course, using the GenElute 96 well Total RNA purification kit (Sigma-Aldrich). cDNA was synthesized using the Transcriptor First Strand cDNA Synthesis Kit (Roche), and quantitative PCR was performed using an ABI 7900 thermocycler (Applied Biosystems) sequence detection system with SYBR green incorporation (Invitrogen, Carlsbad, CA). Relative abundance of template cDNA was calculated by the ΔCt method, normalizing to the abundance of Glyceradelhyde 3-phosphate dehydrogenase (GAPDH) cDNA. Primers for mRNA qPCR analysis were as described previously (*40*). *Egr1* intronic primers were TGATGTCTCCGCTGCAGATC and GGTGGGTGAGTGAGGAAAGG. For phosphorylation at 25 °C, cells were equilibrated at 25 °C for 1h before stimulation. Lysates for SDS-PAGE were prepared in 150 µl 2x SDS sample buffer and treated with Benzonase for 30 min, at 37 °C. Growth rates of TKO cells expressing wild-type and mutant Elk-1 were assessed by plating 2.5×10^4 cells in triplicate for each cell lines, with trypsinization and counting each day over 5 days. For siRNA depletion experiments, cells were transfected with 20 nmol siRNA oligonucleotides using Lipofectamine RNAi MAX (Invitrogen) Control siRNA was All Star (Qiagen). SMARTPOOL mouse MED23 siRNA was from Dharmacon.

Immunoprecipitation, GST-fusion affinity assays, and antibodies

Cells were lysed in PBS, 0.1% NP-40, 1 mM Na_3VO_4, 1mM okadaic acid and protease inhibitor cocktail (Roche Diagnostics), sonicated, and cleared by centrifugation for 15 min at 13000 rpm at 4 °C. For co-immunoprecipitation, lysates were incubated with 20 µl anti-flag M2 magnetic beads for 3 h at 4 °C. For GST-fusion protein affinity assays, 20 µl of gluthatione sepharose beads containing ~10 µg GST fusion protein, with binding for 3 h at 4 °C. Beads were washed 3 times with lysis buffer, and proteins were eluted with 20 µl of 1x SDS loading buffer. Standard transient transfection procedures were used to express HA-MED23 in NIH3T3 cells. Immunoprecipitation and GST fusion protein affinity assays were performed at least three times. Antibodies were: Flag (rabbit), flag M2 peroxidase (HRP), GST (rabbit), Sigma-Aldrich; GFP (rabbit), MCM6

(goat), Santa Cruz Biotechnology; MED23 (mouse), BD Biosciences; MED16 (rabbit), MED24 (rabbit), Bethyl Laboratories; ERK (panERK) (mouse), BD Transduction Laboratories; P-p44/42 MAPK (pERK) (rabbit), phospho-Elk-1(Ser383) (mouse), Cell Signaling; phospho-Elk-1(Thr363) (rabbit) phospho-Elk-1(Thr417) rabbit, in-house (*6*).

Fig. S1.

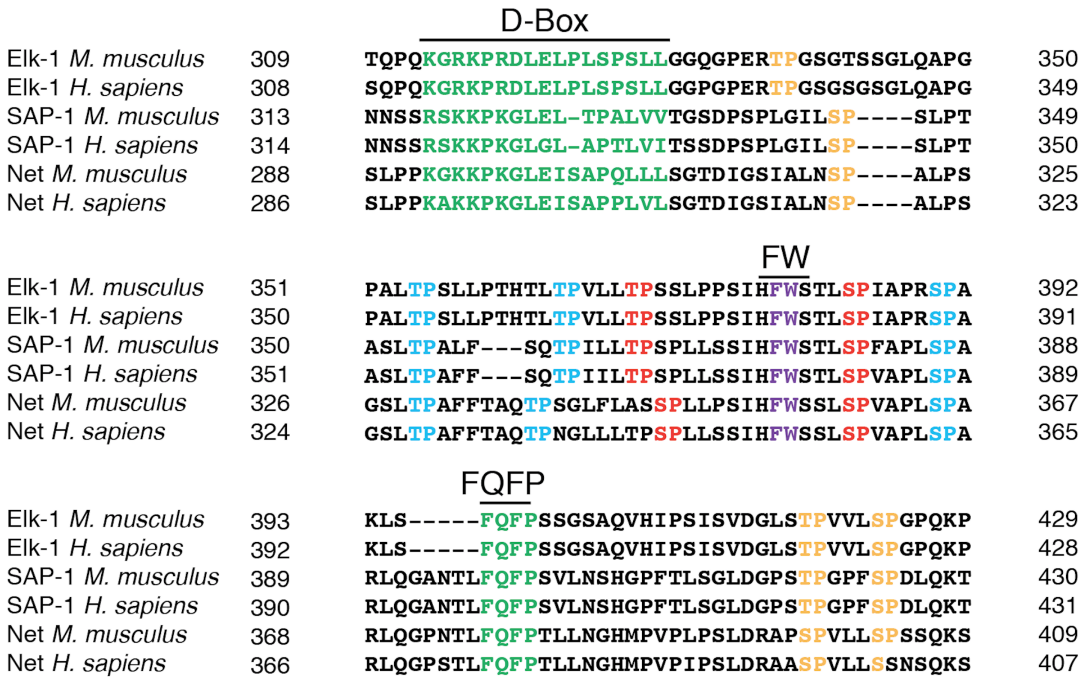

Sequence conservation of human and mouse Elk-1, SAP-1 and Net TADs. Conserved S/T-P phosphorylation sites are highlighted according to Elk-1/ERK2 modification rates as fast, red; intermediate, blue; and slow, yellow. The D-box and FQFP kinase docking motifs are shown in green and the central FW Mediator-binding motif in purple.

Fig. S2

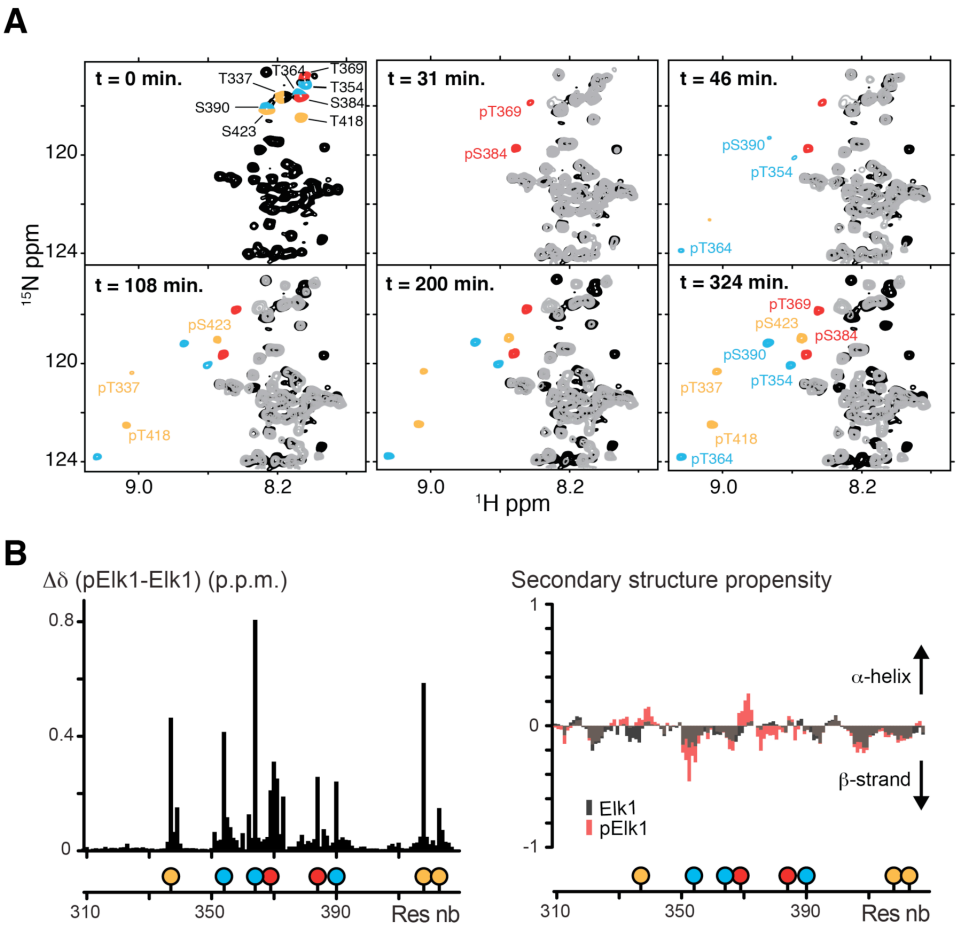

NMR analysis of Elk-1 TAD phosphorylation by ERK2. (**A**) Time-resolved 2D NMR spectra of reconstituted phosphorylation reactions with ^{15}N-labeled Elk-1 TAD (aa309-429) and recombinant, unlabeled ERK2 at indicated reaction time-points. Phospho-site serine-threonine residues are color-coded according to their modification rates, i.e., fast (red), intermediate (blue) and slow (yellow). Progressive appearance of down-field shifted resonance cross-peaks, corresponding to phosphorylated serine-threonine residues, illustrates the time-dependent phosphorylation behavior of individual Elk-1 TAD sites. Grey cross-peaks denote all other Elk-1 TAD residues. (**B**) Left, chemical shift difference (δΔ) analysis between unmodified and phosphorylated Elk-1 TAD with δΔ values plotted for each residue, except prolines, according to (*31*). As expected, Δδ values are highest for phosphorylated Elk-1 TAD residues, with minor changes for neighboring residues, and readily identify modified substrate sites. Right, residue-resolved secondary structure propensity calculations for unmodified (black) and phosphorylated (red) Elk-1 TAD (*32, 33*)using experimentally determined Cα and Cβ chemical shift values as input. As can be appreciated from this plot, overall residual secondary structure propensities are below ~20 % in both forms of Elk-1 TAD and not substantially altered upon multisite phosphorylation. Hence, unmodified and phosphorylated Elk-1 TADs populate structural states that are largely disordered.

Fig. S3

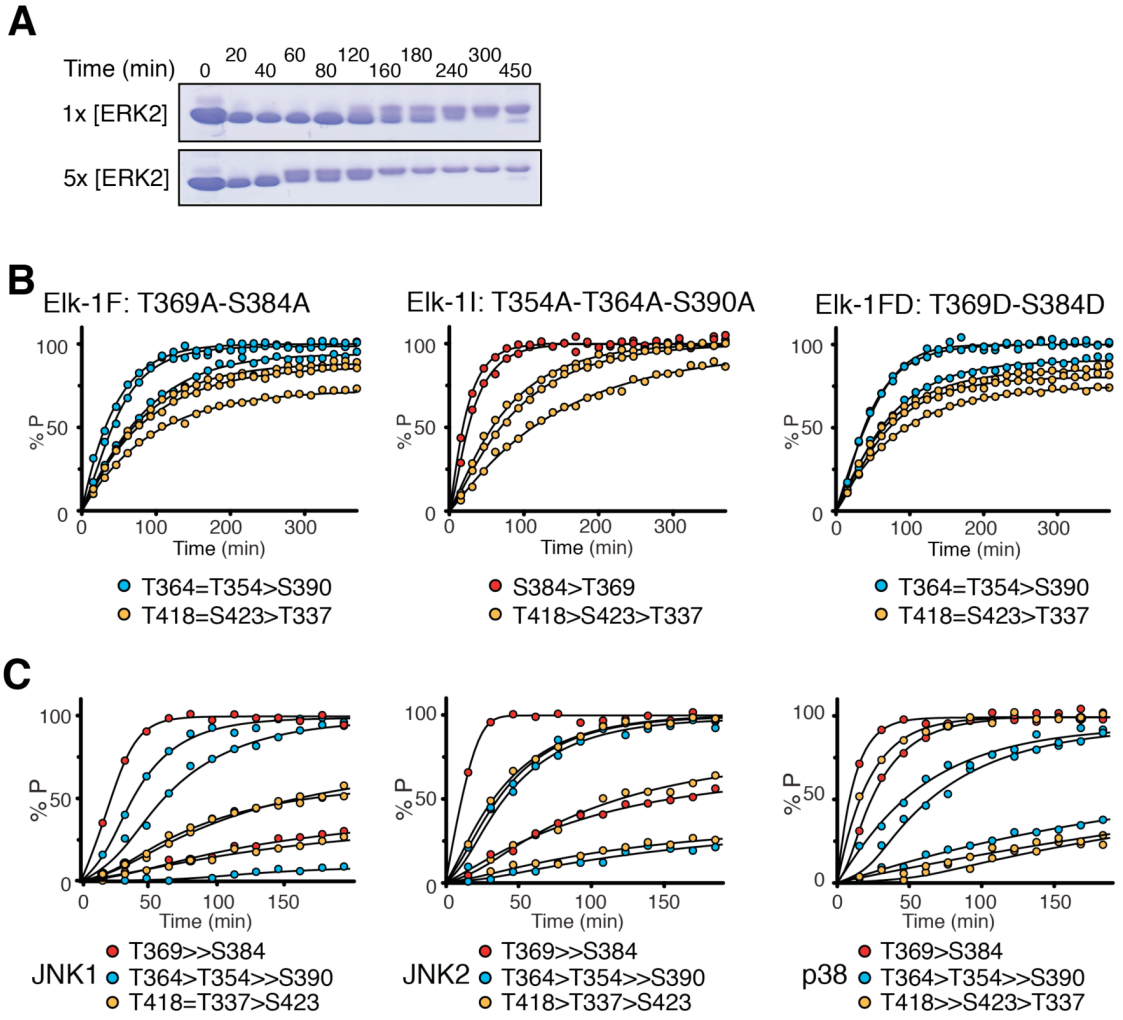

Time-resolved phosphorylation behavior of wild-type and mutant Elk1-TAD (**A**) SDS-PAGE analysis of phosphorylation kinetics of GST-Elk-1 TAD using low and high amounts of ERK2. (**B**) Representative time-resolved modification curves of individual Elk-1 TAD sites upon phosphorylation with ERK2 using fast- (Elk-1F, T369A-S384A) and intermediate-site mutants (Elk-1I, T354A-T364A-S390A) as substrates, as well as fast-site aspartate-substituted Elk-1 TAD (Elk-1FD, T369D-S384D). (**C**) Representative time-resolved modification curves of individual Elk-1 sites upon phosphorylation with JNK1, JNK2 and p38 MAP kinases. Sites are color-coded according to their ERK2 rates. Elk-1 TAD phosphorylation by JNK exhibited a strong kinetic preference for T-P motifs, reminiscent of ERK2 phosphorylation of the FQFP mutant, and consistent with observations showing that JNK does not interact with the FQFP docking site (*14, 15*). TAD phosphorylation by p38 was more similar to ERK2 consistent with p38's ability to interact with FQFP (*25*).

Fig. S4

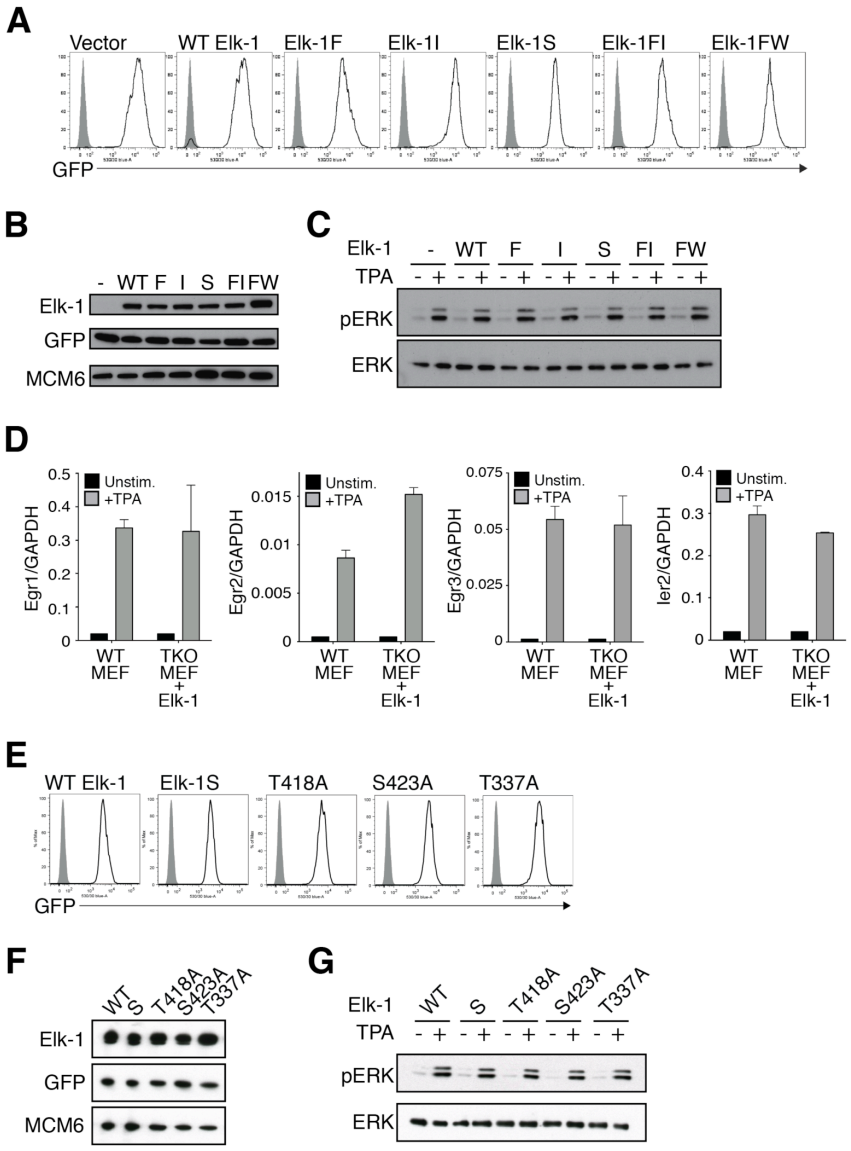

Reconstitution of TCF-deficient MEFs (TKO MEFs) with wild-type or mutant mouse Elk-1. (**A**) Reconstituted TKO cells expressing wild-type Elk-1, Elk-1F, Elk-1I, Elk-1S, Elk-1FI, or Elk-1FW at comparable levels, as confirmed by FACS analysis of the co-expressed GFP marker and (**B**) immunoblotting with anti-Flag antibody. **(C)** ERK activation upon TPA stimulation was comparable in all lines. (**D**) Comparison of TCF-SRF target gene expression in wild-type MEFs and TCF-deficient MEFs (TKO MEFs) reconstituted with wild-type Elk-1. Cells were stimulated with TPA and transcripts quantified by qRT-PCR (relative to GAPDH RNA). Data are mean ± SEM (n=3). (**E-G**) Reconstituted TKO cells expressing wild-type Elk-1, Elk-1S, Elk-1T418A, Elk-1S423A and Elk-1T337A. (**E**) Elk-1 protein levels were comparable, as confirmed by FACS analysis of the co-expressed GFP marker, and (**F**) immunoblotting with anti-Flag antibody (**G**) ERK activation upon TPA stimulation was comparable in all lines.

Fig. S5

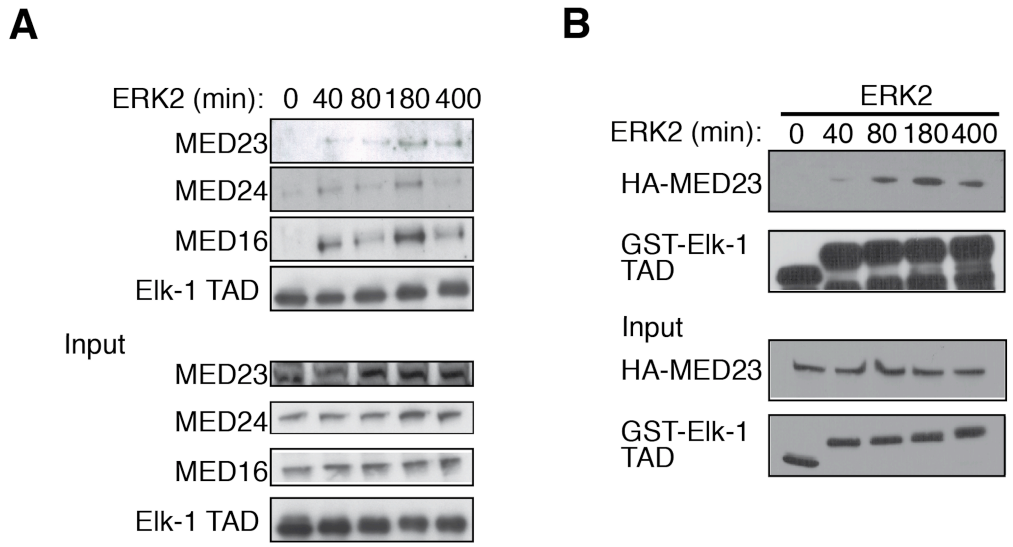

Effect of Elk-1 phosphorylation on Mediator interaction. (**A**) Mediator co-precipitation from unstimulated NIH3T3 cell extracts using wild-type GST-tagged Elk-1 TAD proteins phosphorylated for the indicated times with ERK2, detected by immunoblotting for MED23, MED16 and MED24. (**B**) Affinity precipitation as in (A) but from extracts of NIH3T3 cells transiently expressing HA-MED23.

Fig. S6

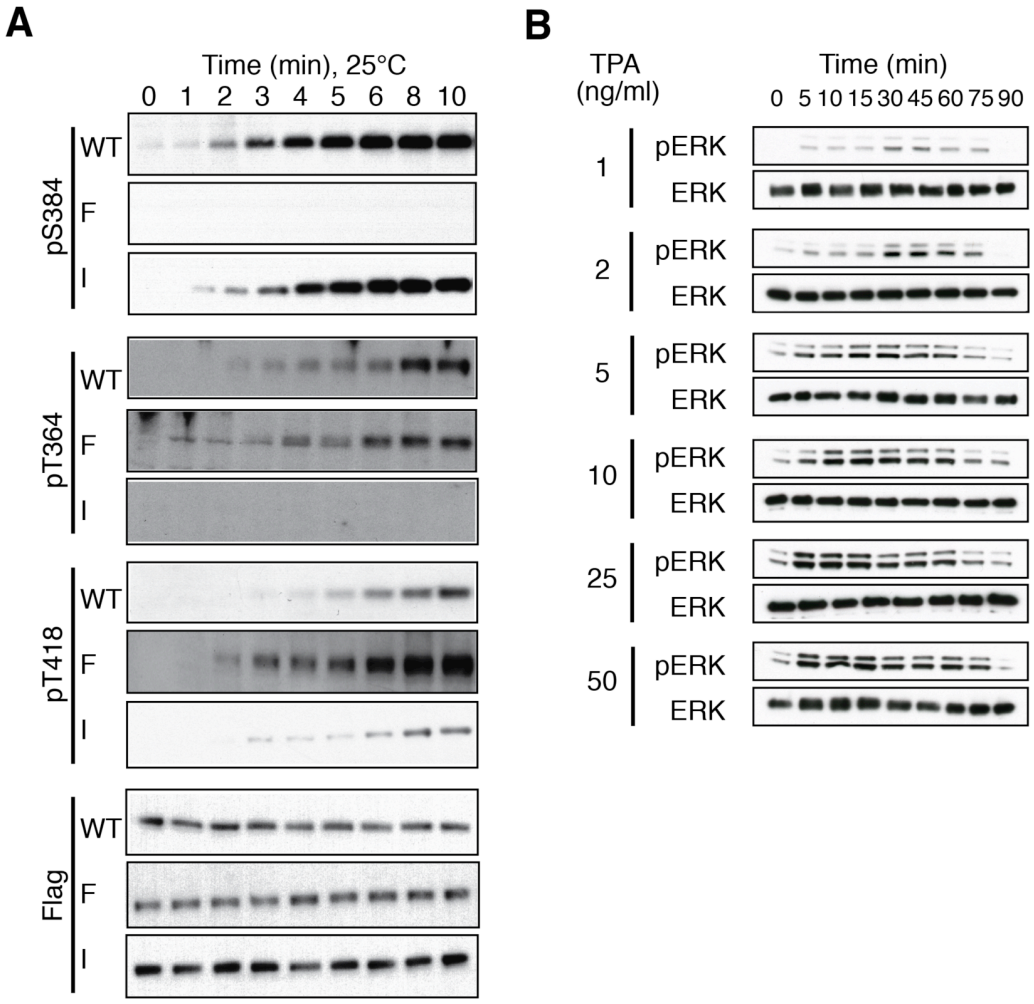

Time course of Elk-1 phosphorylation and ERK activation upon differential TPA stimulation (**A**) Phosphorylation of fast (pS384), intermediate (pT364) and slow (pT418) Elk-1 sites in TCF-deficient MEFs reconstituted with mouse Elk-1 mutants upon stimulation with 50 ng/ml TPA at 25° C. (**B**) Immunoblot analysis of ERK phosphorylation/activation in MEFs reconstituted with wild-type Elk-1 and stimulated with increasing amounts of TPA at 37° C.